Electronic Supplementary Information

Ag-doping effect on MnO_2 cathodes for flexible quasi-solid-state zinc-ion batteries

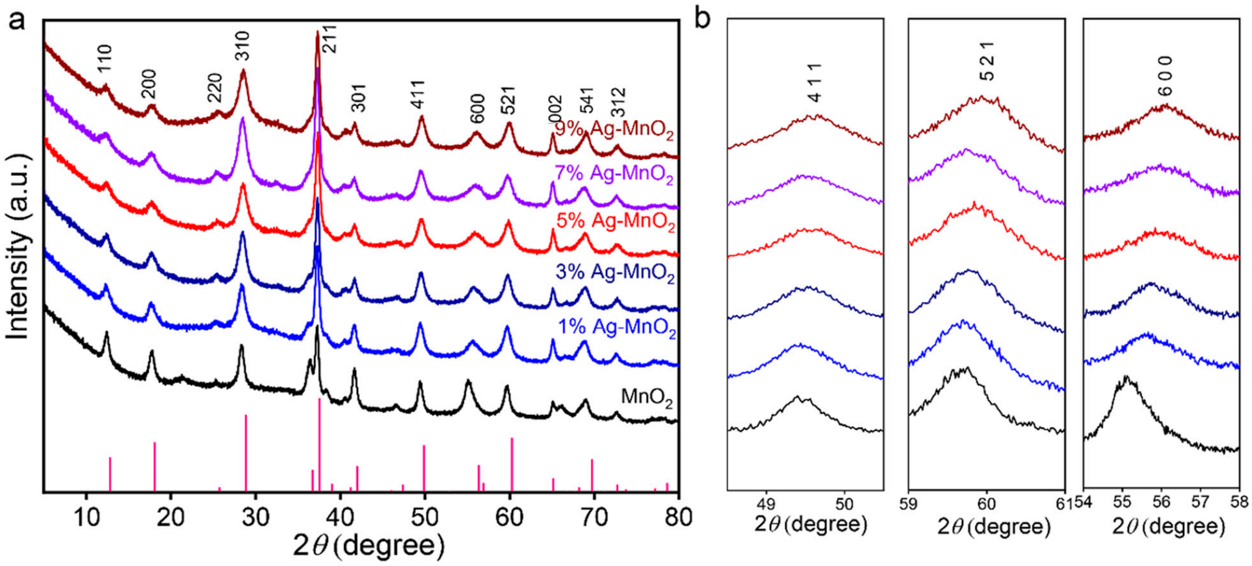

Figure S1. (a) XRD patterns of pure MnO_2 and Ag-doped MnO_2, and (b) the he enlarged view of 411, 521, 600 diffraction peaks.

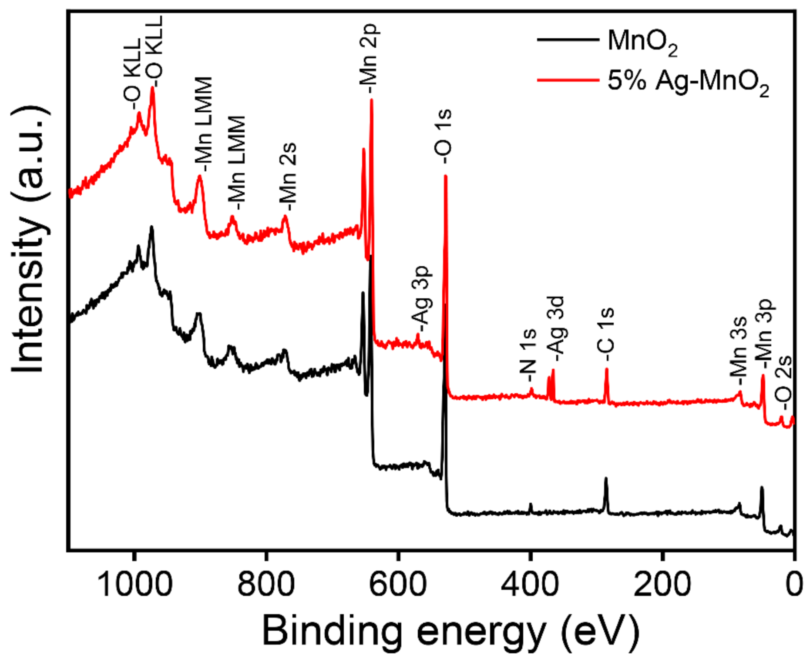

Figure S2. XPS survey spectrum of pure MnO_2 and 5%Ag-MnO_2.

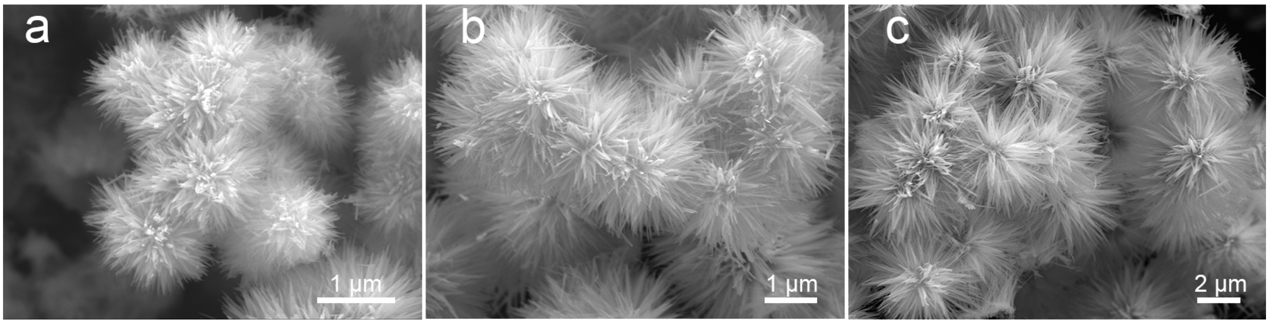

Figure S3. FESEM images of 5%Ag-MnO_2 synthesized at different reaction time of (a) 1, (b) 2, and (c) 4 h.

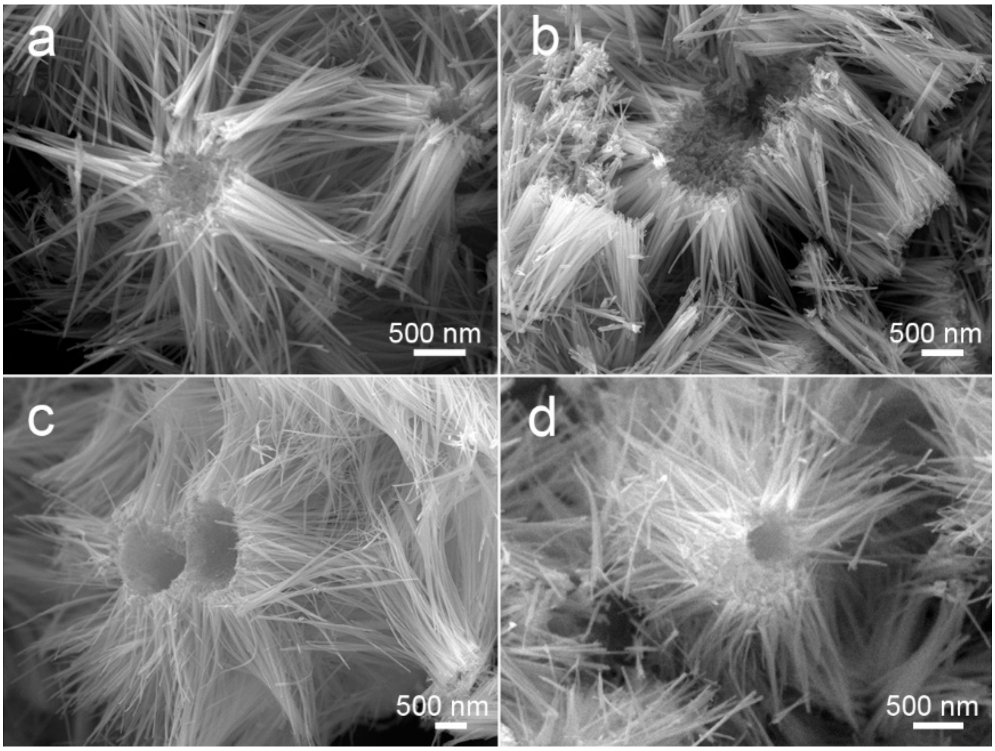

Figure S4. FESEM images of (a) 1%Ag-MnO_2, (b) 3%Ag-MnO_2, (c) 7%Ag-MnO_2, (d) 9%Ag-MnO_2.

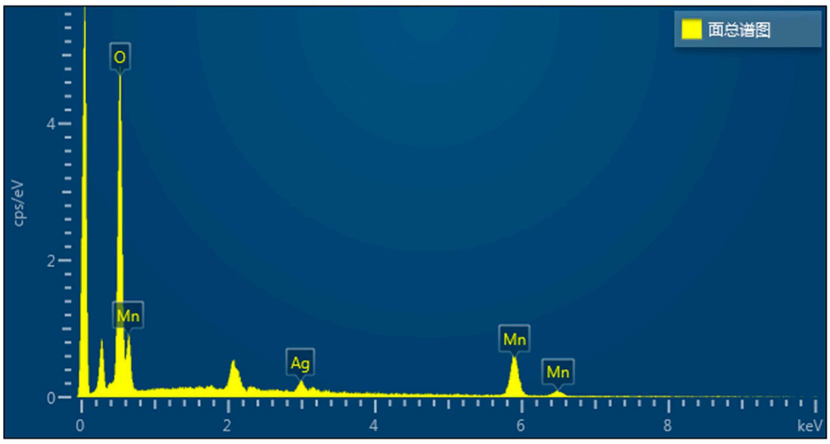

Figure S5. EDS spectrum of 5%Ag-MnO_2.

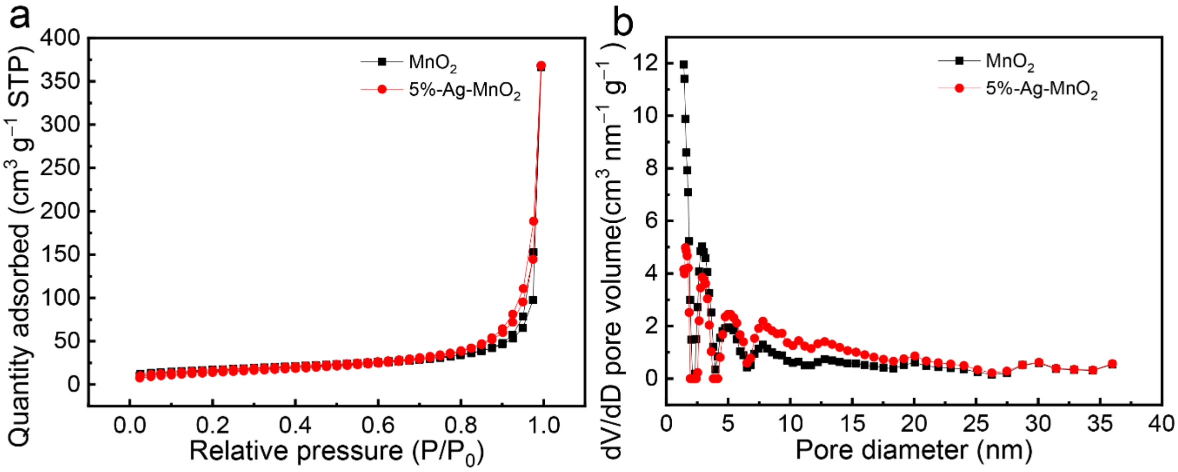

Figure S6. (a) N_2 adsorption–desorption isotherms and (b) pore size distribution curves of pure MnO_2 and 5%Ag-MnO_2.

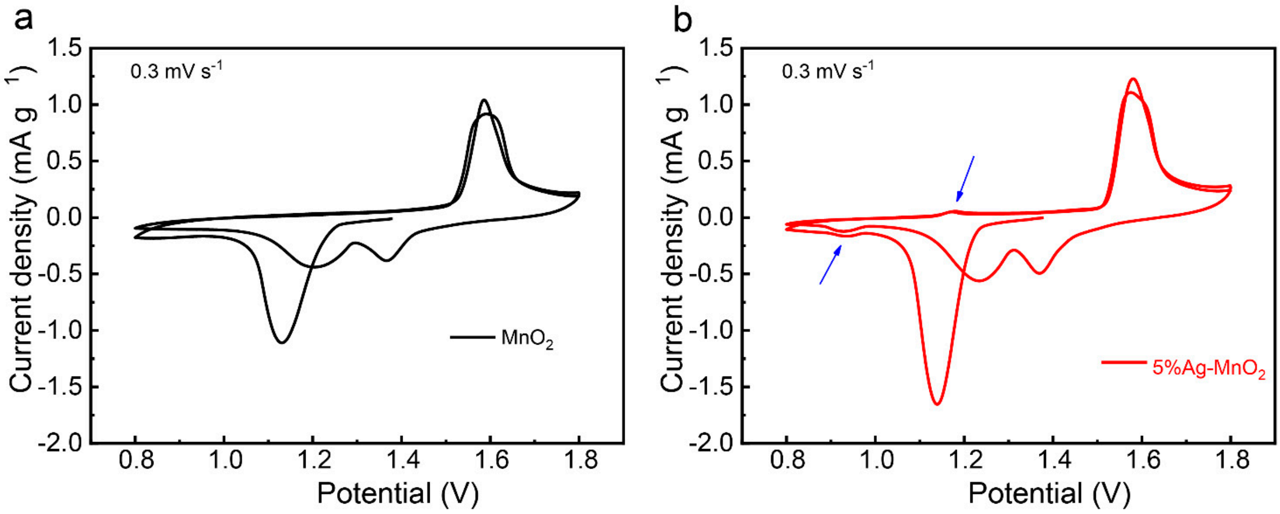

Figure S7. CV curves at a scan rate of 0.3 mV s^{-1} of ZIBs based on (a) pure MnO_2 and (b) 5% Ag-MnO_2.

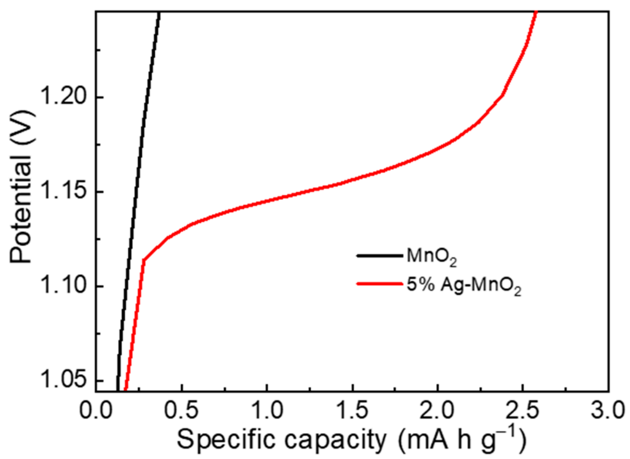

Figure S8. Galvanostatic charge curves of pure MnO_2 and 5%Ag-MnO_2 around 1.15 V.

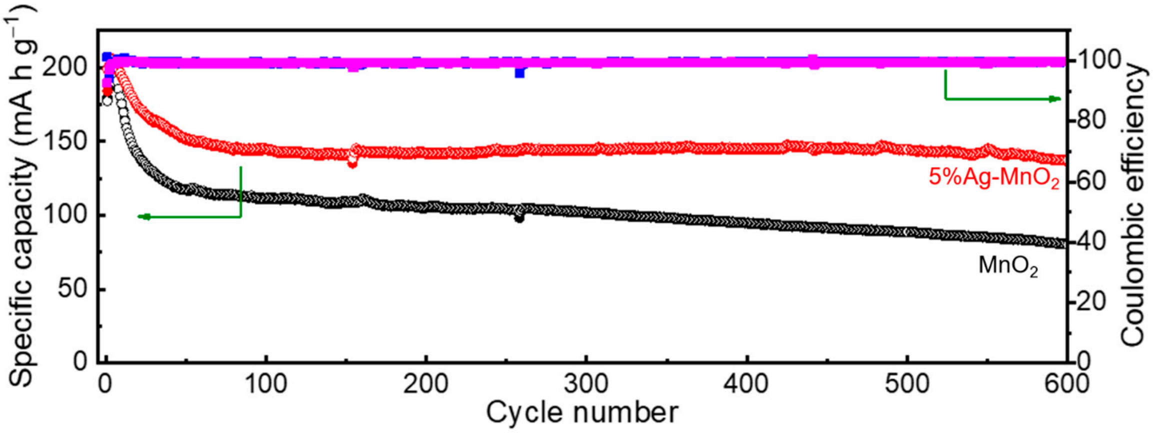

Figure S9. Long-term cycling performance of pure MnO_2 and 5%Ag-MnO_2 at 0.8 A g^{-1}.

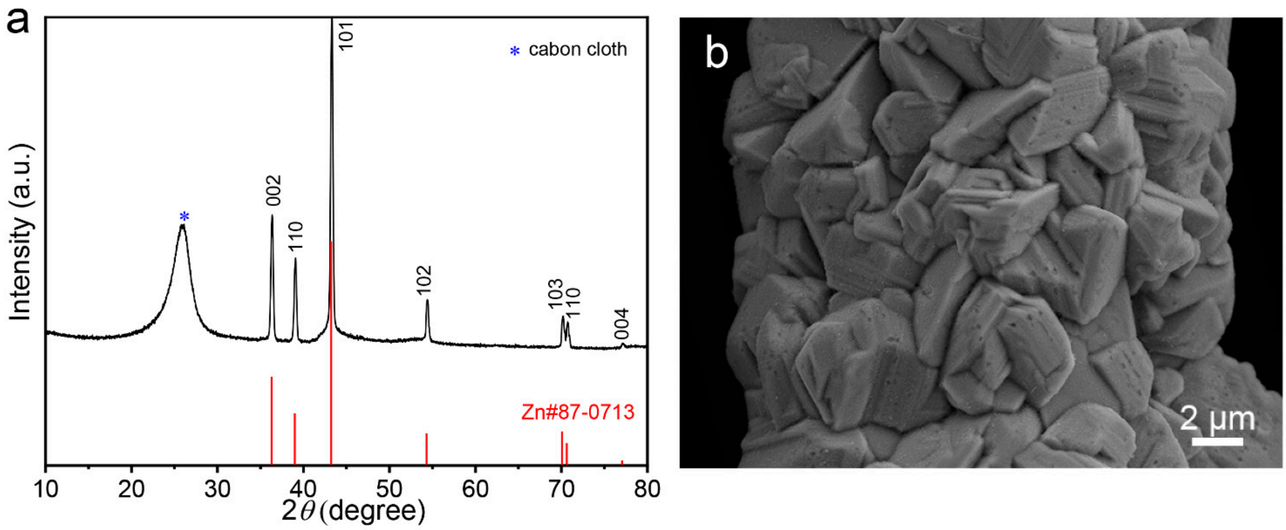

Figure S10 (.a) XRD pattern and (b) FESEM image of the Zn/carbon cloth electrode.

Table S1. Fractional atomic parameters of 5%Ag-MnO_2 with I4/m space group.

atom	site	*x*	*y*	*z*	occupancy
Mn	8h	0.3325	0.1481	0.5	0.9
Ag	8h	0.3313	0.1466	0.5	0.1
O1	8h	0.1717	0.1349	0	1
O2	8h	0.4763	0.1859	0	1

Table S2. Cycling performance of 5%Ag-MnO_2 compared with reported Mn-based cathodes for ZIBs.

Cathodes	Discharge capacity (mA h g^{-1})/ Current density (A g^{-1})	Capacity retention (%)/ Cycles/Current density (A g^{-1})	Reference
α-MnO_2@C	272/0.066	69/50/0.066	[S1]
β-MnO_2	312/0.033	75/200/0.2	[S2]
β-MnO_2	375/0.1	49/1000/0.2	[S3]
$ZnMn_2O_4$	120/0.05	94/500/0.5	[S4]
MnO@NGS	288/0.1	98/300/0.5	[S5]
α-Mn_2O_3	148/0.1	51/2000/2	[S6]
Mn_3O_4	239/0.1	73/300/0.5	[S7]
Amorphous Mn_xO_y	226/0.1	57/200/0.1	[S8]
V-doped MnO_2	266/0.066	49/100/0.066	[S9]
Fe-doped MnO_2	270/0.1	84/100/0.1	[S10]
Ce-doped MnO_2	258/0.15	60/100/1.54	[S11]
N-doped MnO_2	183/0.5	83/1000/5	[S12]
Ag-doped MnO_2	**315/0.05**	**94/500/0.5**	**This work**

Table S3. Cycling performance of our flexible quasi-solid-state ZIB compared with other flexible quasi-solid-state aqueous ZIBs.

Cathodes	Electrolyte	Specific capacity (mA h g^{-1})/ Capacity retention (%)/ Cycles/Current density (A g^{-1})	Reference
MnO_2@CNT	gum	127/-/1000/1	[S13]
MnO_2@CNT	PVA	-/75/300/-	[S14]
ZnHCF@MnO_2	PVA	-/71/500/0.4	[S15]
MoS_2@CC	Starch/PAM	-/97/500/1	[S16]
$LiMn_2O_4$@SS	gelatin	99/90/100/0.025	[S17]
Ag-MnO_2@GP	**PAM**	**171/73/600/1**	**This work**

Reference

S1. Islam, S.; Alfaruqi, M.H.; Song, J.; Kim, S.; Pham, D.T.; Jo, J.; Kim, S.; Mathew, V.; Baboo, J.P.; Xiu, Z.; et al. Carbon-coated manganese dioxide nanoparticles and their enhanced electrochemical properties for zinc-ion battery applications. *J. Energy Chem.* **2017**, *26*, 815-819, doi:https://doi.org/10.1016/j.jechem.2017.04.002.

S2. Islam, S.; Alfaruqi, M.H.; Mathew, V.; Song, J.; Kim, S.; Kim, S.; Jo, J.; Baboo, J.P.; Pham, D.T.; Putro, D.Y.; et al. Facile synthesis and the exploration of the zinc storage mechanism of β-MnO_2 nanorods with exposed (101) planes as a novel cathode material for high performance eco-friendly zinc-ion batteries. *J. Mater. Chem. A* **2017**, *5*, 23299-23309, doi:10.1039/C7TA07170A.

S3. Liu, W.; Zhang, X.; Huang, Y.; Jiang, B.; Chang, Z.; Xu, C.; Kang, F. β-MnO_2 with proton conversion mechanism in rechargeable zinc ion battery. *J. Energy Chem.* **2021**, *56*, 365-373, doi:https://doi.org/10.1016/j.jechem.2020.07.027.

S4. Zhang, N.; Cheng, F.; Liu, Y.; Zhao, Q.; Lei, K.; Chen, C.; Liu, X.; Chen, J. Cation-Deficient Spinel $ZnMn_2O_4$ Cathode in $Zn(CF_3SO_3)_2$ Electrolyte for Rechargeable Aqueous Zn-Ion Battery. *J. Am. Chem. Soc.* **2016**, *138*, 12894-12901, doi:10.1021/jacs.6b05958.

S5. Li, W.; Gao, X.; Chen, Z.; Guo, R.; Zou, G.; Hou, H.; Deng, W.; Ji, X.; Zhao, J. Electrochemically activated MnO cathodes for high performance aqueous zinc-ion battery. *Chem. Eng. J.* **2020**, *402*, 125509, doi:https://doi.org/10.1016/j.cej.2020.125509.

S6. Jiang, B.; Xu, C.; Wu, C.; Dong, L.; Li, J.; Kang, F. Manganese Sesquioxide as Cathode Material for Multivalent Zinc Ion Battery with High Capacity and Long Cycle Life. *Electrochim. Acta* **2017**, *229*, 422-428, doi:https://doi.org/10.1016/j.electacta.2017.01.163.

S7. Hao, J.; Mou, J.; Zhang, J.; Dong, L.; Liu, W.; Xu, C.; Kang, F. Electrochemically induced spinel-layered phase transition of Mn_3O_4 in high performance neutral aqueous rechargeable zinc battery. *Electrochim. Acta* **2018**, *259*, 170-178, doi:https://doi.org/10.1016/j.electacta.2017.10.166.

8. Wu, Y.; Fee, J.; Tobin, Z.; Shirazi-Amin, A.; Kerns, P.; Dissanayake, S.; Mirich, A.; Suib, S.L. Amorphous Manganese Oxides: An Approach for Reversible Aqueous Zinc-Ion Batteries. *ACS Appl. Energy Mater.* **2020**, *3*, 1627-1633, doi:10.1021/acsaem.9b02119.

S9. Alfaruqi, M.H.; Islam, S.; Mathew, V.; Song, J.; Kim, S.; Tung, D.P.; Jo, J.; Kim, S.; Baboo, J.P.; Xiu, Z.; et al. Ambient redox synthesis of vanadium-doped manganese dioxide nanoparticles and their enhanced zinc storage properties. *Appl. Surf. Sci.* **2017**, *404*, 435-442, doi:https://doi.org/10.1016/j.apsusc.2017.02.009.

S10. Xu, J.-W.; Gao, Q.-L.; Xia, Y.-M.; Lin, X.-S.; Liu, W.-L.; Ren, M.-M.; Kong, F.-G.; Wang, S.-J.; Lin, C. High-performance reversible aqueous zinc-ion battery based on iron-doped alpha-manganese dioxide coated by polypyrrole. *J. Colloid Interface Sci.* **2021**, *598*, 419-429, doi:https://doi.org/10.1016/j.jcis.2021.04.057.

S11. Wang, J.; Sun, X.; Zhao, H.; Xu, L.; Xia, J.; Luo, M.; Yang, Y.; Du, Y. Superior-Performance Aqueous Zinc Ion Battery Based on Structural Transformation of MnO_2 by Rare Earth Doping. *J. Phys. Chem. C* **2019**, *123*, 22735-22741, doi:10.1021/acs.jpcc.9b05535.

S12. Zhang, Y.; Liu, Y.; Liu, Z.; Wu, X.; Wen, Y.; Chen, H.; Ni, X.; Liu, G.; Huang, J.; Peng, S. MnO_2 cathode materials with the improved stability via nitrogen doping for aqueous zinc-ion batteries. *J. Energy Chem.* **2022**, *64*, 23-32, doi:https://doi.org/10.1016/j.jechem.2021.04.046.

S13. Zhang, S.; Yu, N.; Zeng, S.; Zhou, S.; Chen, M.; Di, J.; Li, Q. An adaptive and stable bio-electrolyte for rechargeable Zn-ion batteries. *J. Mater. Chem. A* **2018**, *6*, 12237-12243, doi:10.1039/C8TA04298E.

S14. Wang, K.; Zhang, X.; Han, J.; Zhang, X.; Sun, X.; Li, C.; Liu, W.; Li, Q.; Ma, Y. High-Performance Cable-Type Flexible Rechargeable Zn Battery Based on MnO_2@CNT Fiber Microelectrode. *ACS Appl. Mater. Interfaces.* **2018**, *10*, 24573-24582, doi:10.1021/acsami.8b07756.

S15. Lu, K.; Song, B.; Zhang, Y.; Ma, H.; Zhang, J. Encapsulation of zinc hexacyanoferrate nanocubes with manganese oxide nanosheets for high-performance rechargeable zinc ion batteries. *J. Mater. Chem. A* **2017**, *5*, 23628-23633, doi:10.1039/C7TA07834J.

S16. Li, H.; Yang, Q.; Mo, F.; Liang, G.; Liu, Z.; Tang, Z.; Ma, L.; Liu, J.; Shi, Z.; Zhi, C. MoS_2 nanosheets with expanded interlayer spacing for rechargeable aqueous Zn-ion batteries. *Energy Storage Mater.* **2019**, *19*, 94-101, doi:https://doi.org/10.1016/j.ensm.2018.10.005.

S17. Han, Q.; Chi, X.; Zhang, S.; Liu, Y.; Zhou, B.; Yang, J.; Liu, Y. Durable, flexible self-standing hydrogel electrolytes enabling high-safety rechargeable solid-state zinc metal batteries. *J. Mater. Chem. A* **2018**, *6*, 23046-23054, doi:10.1039/C8TA08314B.